Biomaterials. Author manuscript; available in PMC 2018 June 01.

Published in final edited form as:

Biomaterials. 2018 June ; 168: 24–37. doi:10.1016/j.biomaterials.2018.03.044.

Heparin-Poloxamer Thermosensitive Hydrogel Loaded with bFGF and NGF Enhances Peripheral Nerve Regeneration in Diabetic Rats

Rui Li[a,1], **Yiyang Li**[a,1], **Yanqing Wu**[b], **Yingzheng Zhao**[a], **Huanwen Chen**[c], **Yuan Yuan**[a], **Ke Xu**[b], **Hongyu Zhang**[a], **Yingfeng Lu**[d], **Jian Wang**[d], **Xiaokun Li**[b], **Xiaofeng Jia**[e,f,*], and **Jian Xiao**[a,**]

[a]Molecular Pharmacology Research Center, School of Pharmaceutical Sciences, Wenzhou Medical University, Wenzhou, Zhejiang, 325035, China

[b]The Institute of Life Sciences, Wenzhou University, Wenzhou 325035, China

[c]Department of Neurosurgery, University of Maryland School of Medicine, Baltimore, MD 21201, USA

[d]Department of Peripheral Neurosurgery, The First Affiliated Hospital, Wenzhou Medical University, Wenzhou, Zhejiang, 325000, China

[e]Department of Neurosurgery, Orthopaedics, Anatomy Neurobiology, University of Maryland School of Medicine, Baltimore, MD 21201, USA

[f]Department of Biomedical Engineering, Anesthesiology and Critical Care Medicine, The Johns Hopkins University School of Medicine, Baltimore, MD 21205, USA

Abstract

Peripheral nerve injury (PNI) is a major burden to society with limited therapeutic options, and novel biomaterials have great potential for shifting the current paradigm of treatment. With a rising prevalence of chronic illnesses such as diabetes mellitus (DM), treatment of PNI is further complicated, and only few studies have proposed therapies suitable for peripheral nerve regeneration in DM. To provide a supportive environment to restore structure and/or function of nerves in DM, we developed a novel thermo-sensitive heparin-poloxamer (HP) hydrogel co-delivered with basic fibroblast growth factor (bFGF) and nerve growth factor (NGF) in diabetic rats with sciatic nerve crush injury. The delivery vehicle not only had a good affinity for large amounts of growth factors (GFs), but also controlled their release in a steady fashion, preventing degradation in vitro. In vivo, compared with HP hydrogel alone or direct GFs administration, GFs-HP hydrogel treatment is more effective at facilitating Schwann cell (SC) proliferation, leading to

[*]Corresponding author. Department of Neurosurgery, University of Maryland School of Medicine, Baltimore, MD 21201, USA. xjia@som.umaryland.edu (X. Jia). [**]Corresponding author. xfxj2000@126.com (J. Xiao).
[1]These authors contribute equally to this work.

Conflicts of interest

The authors state no conflict of interest.

6. Data availability

The raw/processed data required to reproduce these findings cannot be shared at this time as the data also forms part of an ongoing study.

an increased expression of nerve associated structural proteins, enhanced axonal regeneration and remyelination, and improved recovery of motor function (all $p<0.05$). Our mechanistic investigation also revealed that these neuroprotective and neuroregenerative effects of the GFs-HP hydrogel may be associated with activations of phosphatidylinositol 3 kinase and protein kinase B (PI3K/Akt), janus kinase/signal transducer and activator of transcription 3 (JAK/STAT3), and mitogen-activated protein kinase kinase/extracellular signal-regulated kinase (MAPK/ERK) signaling pathways. Our work provides a promising therapy option for peripheral nerve regeneration in patients with DM.

Keywords

Peripheral nerve injury; Heparin-poloxamer; Basic fibroblast growth factor; Nerve growth factor; Diabetes; Nerve regeneration

1. Introduction

Peripheral nerve injury (PNI) is a worldwide medical problem with substantial socio-economic costs [1,2]. It is predominantly caused by trauma and tumor resections, and altogether affects the quality of life of up to 2.8% of trauma patients [3]. Despite various advances in surgical techniques, recovery from nerve injury remains largely unsatisfactory. Poor outcomes may be correlated with the consistently rising prevalence of chronic illnesses among PNI patients including diabetes mellitus (DM), which is expected to affect 591.9 million patients by 2035 [4]. Long standing hyperglycemia, a common manifestation of DM, significantly complicates treatment outcomes due to its direct impact on nervous system function [5,6], resulting in axonal atrophy, segmental demyelination, and slow regeneration of injured nerves [7,8]. Studies have shown that, compared with normal mice, diabetic mice are more susceptible to deficits in axonal regrowth after acute crush of the sciatic nerve [9], and clinically, treatments capable of inducing complete functional recovery of injured peripheral nerves in diabetics remain elusive. Thus, it is important to seek proper and effective therapies to reduce patient morbidity and financial burden due to PNI.

Growth factors (GFs), a large group of polypeptide therapeutic agents, have been shown to exert cytoprotective and restorative functions on neural repair [10,11]. More specifically, levels of specific GFs are down-regulated in animal models of sciatic nerve injury with diabetes, and administration of exogenous GFs could reverse pathological changes in lesioned nerves by reducing apoptosis and promoting regeneration [12–15]. Among the many GFs that show promise for nerve regeneration, basic fibroblast growth factor (bFGF) and nerve growth factor (NGF) are the most widely studied [16]. bFGF stimulates mitogenesis and proliferation of the dorsal root ganglion (DRG) neurons and Schwann cells (SCs) in vitro [17,18], and also accelerates angiogenesis, remyelination, and synaptogenesis [19,20]. NGF, a thoroughly studied neurotrophin [21], also improves sensorimotor recovery and axonal regeneration [22]. Local injection of recombinant NGF also attenuates nerve regeneration deficits due to diabetic neuropathy by up-regulating neuritin levels [23].

While growth factors are potent stimulators of nerve regeneration, growth factor therapy remains insufficient for adequate recovery from PNI largely due to their rapid degradation and redistribution in vivo [24,25]. Thus, employing a suitable delivery vehicle that not only maintains the GFs' bioactivity and bioavailability but also controls their spatiotemporal release is particularly important. Our previous studies have demonstrated that thermosensitive heparin-poloxamer (HP) hydrogel is biocompatible and improved the bioavailability of GFs [26]. Its ingredient, heparin, showed high affinity to a variety of GFs [27], allowing it to carry bFGF and NGF to cell-surface receptors to enhance intracellular signal transduction. Furthermore, while GFs have shown convincing efficacy when administered alone with/without biomaterials [22,23,28,29], the regeneration of injured peripheral nerves is a dynamic process that requires several GFs and cytokines to stimulate axonal outgrowth and remodeling of the intracellular cytoskeleton [30], so single GF administration are unlikely to adequately satisfy the curative demands of patients with multi-illnesses [31].

In the present study, for the first time, we loaded both NGF and bFGF onto an HP hydrogel to form a [HP:(bFGF + NGF)] hydrogel (collectively called GFs-HP), and used this vehicle to deliver multi-GFs in situ to diabetic rats with sciatic nerve injury. Hydrogel micromorphology, rheology and cumulative release rate were monitored and characterized in vitro using scanning electron microscopy (SEM), coaxial cylinder rheometer and ELISA. Then, GFs-HP hydrogel was administered in situ to rat sciatic nerve lesions using a micro syringe, and SC proliferation, axonal regeneration, functional outcomes, and mechanisms of action were evaluated by morphological, pathological and functional assessments.

2. Materials and methods

2.1. Preparation of GFs–HP hydrogels

First, the synthesis of heparin-poloxamer (HP) was performed according to the 1-Ethyl-3-(3-dimethyl aminopropyl) carbodiimide/N-Hydroxyl succinimide (EDC/NHS) method [32]. Briefly, poloxamer 407 (Badische Anilin Soda Fabrik Ga, Shanghai, China) reacted with 1.3mM 4-nitrophenyl chloroformate and diamino ethylene to obtain a mono amine-terminated Poloxamer (MATP). Then, this intermediate was coupled with heparin salt by EDC and NHS in 2-(N-morpholine) sulphonic acid (MES) buffer for 1 day at 25°C. The reactive mixture was dialyzed for 3 days and lyophilized to obtain HP powder. Next, GFs-HP hydrogels were prepared using the cold method. Briefly, lyophilized HP powder was dissolved in fresh saline (4°C) to obtain the original hydrogel solution with 6.4×103mg/ml, and then added to the bFGF and NGF original solution (30mg/ml and 45mg/ml, respectively; Key Laboratory of Biotechnology and Pharmaceutical Engineering, Wenzhou Medical University, China) at 4°C under gentle stirring. The final concentrations of bFGF, NGF and HP polymer was 1mg/ml,1mg/ml and 160mg/ml, respectively. (These concentrations ensure complete incorporation of bFGF and NGF in HP (Supplemental Fig. 1A)). The preparation of GFs-HP hydrogels was performed under the aseptic conditions. The final mixture was stored at 4°C overnight to form clear colored GFs loaded hydrogel solution.

2.2. Characterization of GFs-HP hydrogels

Rheological measurements of HP and GFs-HP were tested in a coaxial cylinder rheometer (DV-III, Brookfield, U.S.) at different temperatures from 10 to 40°C. The elastic modulus and viscous shear modulus were measured using stainless steel parallel flat plates (25mm), and rheological curves were plotted against temperature. The micromorphology of the dried samples was observed by scanning electron microscopy (SEM, Hitachi H-7500, Japan). The dehydrated specimens were cross-sectioned and sputter-coated with gold followed by scanning observation.

2.3. Release profile of bFGF/NGF from GFs-HP hydrogels

At predetermined time points (1d, 3d, 7d, 14d, 21d, 28d and 35d), supernatant from the GFs-HP containing GFs were collected and replaced by an equal volume of fresh medium. Then, GF release was analyzed by specific GF enzyme-linked immunosorbent assay kit (ELISA, Westang system, Shanghai, China) and absorbance was measured at 450nm with a microplate reader.

2.4. Effects of HP on RSC 96 survival in vitro

RSC 96SCs (Sciencell, Shanghai, China) were cultured in 6-well plates (100,000cells/well) in Dulbecco's modified Eagle Medium (DMEM) containing 1% penicillin/streptomycin solution (P/S) and 10% fetal bovine serum (FBS) (Gibco, USA) in a humidified incubator (37°C, 5% CO_2). 24h later, the original medium was discarded and replaced with fresh medium (control), or medium containing HP hydrogel with/without GFs (100ng/ml bFGF and NGF) for another 48h, and the apoptosis of SCs was analyzed using Annexin V-fluorescein isothiocyanate (Annexin V-FITC)/Propidium iodide (PI) staining to investigate early apoptosis as previously described [33]. Fluorescence intensity was analyzed via flow cytometry (BD, Biosciences).

2.5. The stability evaluation of the GFs in the hydrogel

PC12cells (Sciencell, Shanghai, China) were seeded and cultured on 96-well plates at the density of 5000cells per well for 24h. After removing medium and washing with PBS, the PC12cells were treated with free bFGF or NGF (100ng/ml), or HP hydrogel containing the same amount of single GFs (the prepared NGF-HP and bFGF-HP were placed in 37°C for 10, 20, and 30 days) in medium for another 48h. Then, cells were incubated in medium with 10μl of CCK-8 solution for 2h. Absorbance was measured at 450nm using a microplate reader (Bio-Rad, CA, USA).

2.6. Animal model and orthotopic injection

Male SD rats (200–220g) were obtained from the Laboratory Animals Center of Wenzhou Medical University. The living conditions and experimental procedures conformed to the National Institutes of Health (NIH) Guide Concerning the Care and Use of Laboratory Animals. All animal experiments described were approved by the Animal Experimentation Ethics Committee of Wenzhou Medical University, Wenzhou, China. Prior to the beginning of in vivo experiments, animals were maintained for at least 7d to adjust to the standardized laboratory temperature (23±2°C), humidity (35–60%), and a light-dark cycle (12:12h).

40 animals were used in total, and were initially divided into two groups: Control (n=8), and Diabetes (n=32). Prior to any procedures, diabetes was induced in rats in the Diabetes group by intraperitoneal injection of streptozotocin (STZ) with a dose of 65mg/kg in phosphate-buffered saline (PBS), and rats in which blood glucose concentration ≥16.7mmol/L after 7d were considered to have DM [34]. The control group received an equal volume of PBS. The values of blood glucose in the control groups and STZ-diabetes rats were 6.18±0.33 and 20.50±0.95mmol/L, respectively.

4 weeks after initiation of diabetes, Diabetes rats were anesthetized by an intraperitoneal injection of 10% chloral hydrate (3.5ml/kg). Crushed injuries of sciatic nerves were administered to the Diabetes group according to a previously described method [35]. In brief, after an appropriate incision of the skin, the gluteal musculature was separated in order to expose the right sciatic nerve. The exposed nerve 7mm proximal from sciatic notch was subject to crush using two vascular clips (Oscar, China) at two ends with 30g force for 2min. Control group animals received the same surgical procedures for anesthesia and skin and muscle operations, but without sciatic nerve crush injury.

Following sciatic nerve crush injury, the diabetes rats were further divided into four groups (n=8 for each): PNI-diabetes, HP hydrogel, Free GFs and GFs-HP hydrogel. For the GFs-HP hydrogel group, GFs–HP hydrogels were administered via single dose orthotopic injection at a dose of 15μl through a micro syringe. Similarly, the HP hydrogel group received a single orthotopic injection of GFs-free hydrogel (OI). As for the free GFs group, 500ng bFGF and 500ng NGF were mixed and injected in situ at the right hindlimb for 30 consecutive days. The rats in the PNI-diabetes group received the same dose of saline. 30 days after treatment, rats were sacrificed, 5 rats were randomly selected for various pathological studies, and the crushed nerves and corresponding gastrocnemius muscles were harvested for assessment.

2.7. BBB score assessment

Rat hindlimb patterns of recovery after sciatic nerve contusion injury was evaluated using the Basso, Beattie, and Bresnahan (BBB) scores. BBB is widely used to assess functional recovery in spinal cord injured animals, and has also been demonstrated to be valuable in assessing nerve repair in peripheral nerve injuries [36,37]. Two trained investigators who were blind to the experimental conditions scored hindlimb movements in an open field at 1, 3, 7, 14 and 28 days post-operation. BBB is a 22-point scale (scores 0–21) that reflect the recovery of hindlimb locomotion recovery from a score of 0, indicative of no recovery of the movement in the hindlimb junctions, to 21, representative of a normal ambulating rodent.

2.8. Analysis of walking tracks

Animals are tested in a confined walkway (an 8.2cm wide by 42cm long white paper) with a dark shelter at the end. Individual ink footprints were recorded on the white paper after rats walked through the corridor. Three different parameters including PL (distance from the heel to the third toe), TS (distance from the first to the fifth toe) and IT (distance from the second to the fourth toe) were evaluated via the following formula for sciatic function index (SFI; derived by Bain et al. [37]):

$$\mathrm{SFI} = -38.3 \times (\mathrm{EPL} - \mathrm{NPL})/\mathrm{NPL} + 109.5 \times (\mathrm{ETS} - \mathrm{NTS})/\mathrm{NTS} + 13.3 \times (\mathrm{EIT} - \mathrm{NIT})/\mathrm{NIT} - 8.8$$

Schematic for measuring parameters of footprints is shown in Fig. 3D. E is the experimental side and N is the normal side. An SFI equal to −100 indicates total impairment, whereas an SFI oscillating around 0 is considered to reflect normal function. Two observers, unaware of the experimental procedures, performed the test from day 1 to day 28 following surgical procedures.

2.9. Histological assessment of nerve and muscle

Bilateral gastrocnemius muscles were harvested and wet weights were measured as described before [38,39]. The muscle wet weight ratio (%) was calculated as: the muscle wet weight of the injured limb/the weight of the contralateral one×100%. Muscle morphology were assessed in 10μm thick sections with H&E staining. Representative images were selected for analyzing muscle fiber using the software Image-Pro Plus (version 6.0, Media Cybernetics, Inc., MD, USA). The atrophy ratio of the gastrocnemius muscle was calculated as following equation: the atrophy ratio=the gastrocnemius muscle fiber area/the total image area×100% [54]. The longitudinal sections of the nerve samples were cut in 5μm thicknesses for masson’s trichrome staining (Beyotime). Sections were analyzed, and images were captured using a Nikon ECLPSE 80i camera (Nikon, Japan).

2.10. Transmission electron microscopy

The myelin sheath regeneration post-contusion at 30 days was detected by a transmission electron microscope (TEM, H7650, Hitachi, Tokyo, Japan). The fabrication of ultra-thin (50nm) sections of sciatic nerves, image capturing procedure, and quantification of morphometric data were performed as previously described [35].

2.11. Immunoblotting

2-cm length of regenerated nerve segment were extracted in separate pooled protein lysates. After protein concentration in each sample was quantified with Carmassi Bradford reagents (Thermo, Rockford, IL, USA), 50μg of protein were separated by SDS-PAGE and transferred onto PVDF membranes (Millipore, Bedford, MA). The following primary antibodies were used: Ace-tubulin (1μg/ml, T7451, Sigma), Tyr-tubulin (1μg/ml, ab6046, Abcam), Tau (1μg/ml, ab18207, Abcam), GAP43 (0.67μg/ml, sc-17790, Santa), PCNA (0.67μg/ml, sc-25280, Santa), Ki67 (1μg/ml, ab15580, Abcam), *p*-AKT (1μg/ml, ab183758, Abcam), AKT (0.67μg/ml, sc-8312, Santa), *p*-ERK (0.67μg/ml, sc-7383, Santa), ERK (0.67μg/ml, sc-292838, Santa), *p*-STAT3 (1μg/ml, ab76315, Abcam), STAT3 (1μg/ml, ab68153, Abcam) and GAPDH (0.1μg/ml, AP0063, Bioworld). Signals were detected by chemiluminescence using gel imaging system (Bio-Rad Laboratories, Hercules, CA, USA). Density values were normalized to GAPDH and results are representative of five independent experiments.

2.12. Immunofluorescence evaluation

Standard immunohistochemistry procedures are described previously [35], and the following primary antibodies were used: anti-MBP (myelin marker, 1μg/ml, ab40390, Abcam) and anti-NF200 (heavy subunit of neurofilament for axons, 0.01μg/ml, ab4680, Abcam), anti-GFAP (SCs, 0.67μg/ml, sc-6170, Santa) and anti-Ki67 (marker for cell proliferation, 1μg/ml, ab15580, Abcam). All images were captured on an inverted confocal microscope (Nikon) or a Nikon Eclipse 80i fluorescence microscope. The percentages of MBP and NF200 positive areas were calculated by dividing Integrated option density (IOD, 6 randomly selected middle-power fields in each animal) by selected region area, then multiplied by 100%. All parameters were measured using Image-Pro Plus (images threshold: H (0–30), S (0–255) and I (0–230)).

2.13. Statistical analysis

All numerical data were presented as mean±SEM. Walking track test was compared using two-way repeated measurements analysis of variance (ANOVA). The Kruskal–Wallis ANOVA on Ranks was applied with Dunn's method to test BBB scores. Data from immunoblotting and immunofluorescent evaluation were validated using one-way ANOVA with Bonferroni's multiple comparisons for post-hoc analysis. All statistical analyses were performed with statistical software SPSS 21.0 (SPSS Inc, Chicago, IL, USA) and GraphPad Prism software Version 5 (GraphPad Software, Inc, San Diego, CA) and $P<0.05$ was considered statistically significant.

3. Results

3.1. HP hydrogels loaded with GFs retain thermal-sensitive characteristics

Our purchased Poloxamer 407 and synthetic HP are highly pure copolymers with the weight-average molecular weight (Mw) of ~10.6 KD and ~18.7 KD, respectively (Supplemental Fig. 1B and C). The block ratio of Poloxamer 407 to Heparin are estimated to be 44% (Supplemental Fig. 1D). To achieve a suitable gelation temperature for restoration surgery at body temperature, we prepared a HP so lution concentration of 17% (w/w) for this research, which has been demonstrated to be the most suitable in prior studies [40]. As shown in Fig. 1A, HP was a liquid at 4°C, but it quickly transitioned to the hydrogel (gel) state after heating to 37°C, and it transitioned back to a solution (sol) state again after the temperature returned to 4°C. We further explored phase transition temperature of this thermosensitive HP by rheology tests. In this experiment, two gelatinous parameters, storage modulus (G') and loss modulus (G''), respectively reflect the change of viscosity and elasticity. The G', G'' values of the HP hydrogel increased rapidly under the temperature between 17 and 22°C (Fig. 1B), indicating a process of sol-gel phase transition. Thus, it can easily form gels under body temperature (37°C). There were unchanged sol-gel-sol phase transitions under the same three temperature points after mixing bFGF and NGF to the HP (Fig. 1C). However, the phase transition temperature of GFs-HP decreased to 14 – 19 °C (Fig. 1D), which was a slight difference from HP alone. This may be due to micelle packing and entanglements of poloxamer 407 being disturbed after incorporating bFGF and NGF. Overall, this gelation process demonstrated that GFs-HP has a preferable phase change temperature, which is particularly suitable for in vivo treatment and drug delivery to repair nerve damage.

3.2. The 3D porous structure of GFs-HP is safe and persistently maintains GFs stability

The micromorphology of dehydrated HP-based hydrogels was investigated by SEM (Fig. 2A). The results showed a highly aligned porous structure resembling a cribriform plate in the blank hydrogel. Moreover, the porous structure on the surface was interconnected. For GFs-HP hydrogel, we also observed similar porous domains. Structures are shown with higher resolution with higher magnification (Supplementary Fig. 2). These observations suggest that HP hydrogels are suitable for GFs' absorption and retention. To further determine the safety of GFs-HP hydrogel, RSC96cells, a rat Schwann cell (SC) line, were cultured in the medium with HP containing with/without GFs. The result of Annexin V^+/PI^- showed no obvious difference on early apoptotic rate between GFs-HP and HP groups via Fluorescence Activated Cell Sorting (FACS), and was consistent with the SC cultured in normal medium (Fig. 2B, control group: 1.69±0.08, vs. GFs-HP group: 1.48±0.05, P =0.124), suggesting that the ingredient of HP in the GFs-HP hydrogel did not impact RSC 96cell survival. We next investigated the stability of the bFGF and NGF in the HP hydrogel within 30 days. From the CCK-8 results, it was demonstrated that NGF and NGF-HP both significantly increased cell viability, but there was no significant difference in cell viability between NGF and NGF-HP (Fig. 2C). This trend was also confirmed when comparing bFGF and bFGF-HP. These results indicate that NGF and bFGF are incorporated in HP without deactivation over time, and maintains stability over 30 days.

3.3. Controlled release of bFGF and NGF from GFs-HP persistently improves motor functional recovery of PNI-diabetic rats

In vitro release profile of NGF/bFGF-HP hydrogel showed an initial rapid phase for both GFs over the first week, followed by a slow and nearly linear phase during the rest of the detection time points, with 35% of bFGF and almost 48% of NGF being released by day 35 (Fig. 3A). This indicated that GFs-HP hydrogels controlled the release of incorporated two GFs well. To evaluate whether the sustained-release of bFGF and NGF from the GFs-HP coincides with locomotor recovery, the walking tracks and BBB rating scale at indicated time points were evaluated. Results revealed that the SFI value and BBB score displayed no obvious difference among the four injured groups during the first week. At week 2 after the operation, these scoring parameters in the GFs treatment groups showed improvements when compared with the no GFs treatment groups, with the GFs-HP group showing significantly higher scores than PNI-diabetes group (− 59.65 ± 4.01 vs. − 77.62 ± 3.94, P =0.007 for SFI and 14.63±0.73 vs. 11.25±0.45, P=0.002 for BBB). At 4 weeks post-operation, this difference became more pronounced, and the motor functional recovery in the GFs-HP hydrogel group was clearly superior to that of free GFs group (Fig. 3B and C, − 31.34 ± 3.71 vs. − 47.62 ± 4.28, P=0.013 for SFI and 18.50±0.60 vs. 16.38±0.42, P =0.014 for BBB), manifesting the best per formance. Photographic evaluation visibly indicated unambiguous footprints with the most superior toe spread in the GFs-HP group when compared other groups, almost resembling the control group (Fig. 3E). These results indicated that sustained-release mediated by HP hydrogel was able maintain bFGF and NGF at an efficient and stable concentration in the contusion region, which led to effective restoration of motor function in the PNI-diabetic rats.

3.4. GFs-HP hydrogel attenuates gastrocnemius muscle atrophy after injury

30 days after the repair, the gastrocnemius muscles of both hind limbs in all groups were separated, and wet weight and atrophy were analyzed. Fig. 4A showed the gross images of the isolated gastrocnemius muscles in the injured side were obviously atrophic when compared with the contralateral side in all four surgery groups, and was especially pronounced for the PNI-diabetics group. HE staining showed that when compared with GFs or HP-hydrogel groups, the degree of muscle atrophy in GFs-HP group was obviously attenuated, resulting in larger muscle fibers with well-defined organization (Fig. 4B and C. GFs-HP group: 83.37±2.86%, vs. PNI-diabetics group: 55.85±2.76%, $P < 0.001$; GFs-HP group: 83.37±2.86%, vs. Free GFs group: 70.46±2.42%, $P = 0.011$). Similarly, the relative wet weight of the gastrocnemius muscles in the GFs-HP hydrogel group was significantly higher than that of the GFs group and other surgery groups (Fig. 4D. GFs-HP group: 89.41±2.75%, vs. PNI-diabetics group: 55.16±4.40%, $P < 0.001$; GFs-HP group: 89.41±2.75%, vs. Free GFs group: 74.40±3.26%, $P = 0.017$). Taken together, these results suggest that the HP hydrogel incorporating bFGF and NGF maintains the morphology of muscle fibers and prevents atrophy after sciatic nerve injury.

3.5. GFs-HP hydrogel stimulates axonal regeneration and remyelination

Masson trichrome staining (MTS) was used to evaluate the regenerated nerves of the longitudinal sectionsat 30 days. Results of histological evaluation showed the number and arrangement of nascent nerve fibers in the PNI-diabetes and HP-hydrogel groups were scarce and disorganized. On the contrary, the GFs group and GFs-HP group showed a large number of myelinated nerve fibers with oriented growth and clear outlines. Moreover, the GFs-HP group nearly approximated to that of the Control group (Fig. 5A). TEM was also used for visualizing myelin sheath regeneration. Consistent with the result of MTS, at 30 days postoperatively, most regenerated axons were encased by thick electrondense myelin sheaths in the Free GFs and GFs-HP groups, while the myelin sheath regeneration in PNI-diabetes and HP-hydrogel groups remained thin, loose, and exhibited vacuolar-like defects which were typical features of demyelination (Fig. 5B). Statistical analysis of myelinated axonal counts also showed that the GFs-HP group was significantly superior to other treatment groups (Fig. 5D, from 469±14 in the GFs-HP to 374±16, 275±29, and 267±29 in Free GFs, HP hydrogel and PNI-diabetics, respectively. GFs-HP group vs. Free GFs group, $P = 0.003$; GFs-HP group vs. PNI-diabetes group, $P < 0.001$), and its G-ratio was the smallest (Fig. 5E, the rankings were 0.83±0.02 > 0.82±0.02 > 0.68±0.03 > 0.56±0.04 in the four crushed groups for PNI-diabetics, HP hydrogel, Free GFs, and GFs-HP groups, respectively. GFs-HP group vs. Free GFs group, $P = 0.047$; GFs-HP group vs. PNI-diabetes group, $P < 0.001$).

To further investigate the effects of GFs-HP on nerve regeneration, we performed immunohistochemical staining on longitudinal nerve sections stained with an antibody against Myelin basic protein (MBP, representing myelination) and Neurofilament 200 (NF-200, marked for neurofilaments for axonal tracing). The result of co-staining showed that MBP was densely and regularly distributed along the NF-200 in the Control group. The number and distribution of myelin and neurofilament in the PNI-diabetics and HP-hydrogel groups were scarce and disorganized, indicating a severe remyelination defect, while in the Free GFs or GFs-HP groups, the presence of myelinated axons was evident (Fig. 5C). Quantitative analysis of NF-200 and MBP expression showed that the Free GFs group had significantly higher levels than the PNI-diabetes and HP-hydrogel groups, but were inferior to the GFs-HP hydrogel group (Fig. 5F and G. 54.17±1.78% vs. 39.30±2.40%, P=0.002 for MBP and 42.04±2.37% vs. 32.68±1.19%, P=0.017 for NF-200). These data indicated that co-delivery of bFGF and NGF were favorable for axon outgrowth and remyelination after sciatic nerve damage.

3.6. GFs-HP augments microtubule stabilization and functional protein secretion

Microtubules (MTs) are polar constituents of the cell cytoskeleton, participate in growth cone steering and extension, and play a pivotal role in axon formation [41]. MT stability and dynamics are regulated by combined actions of several classes of intrinsic proteins, including acetylated a-tubulin (Ace-tubulin) and tyrosinated a-tubulin (tubulin) [42]. The ratio of Ace-tubulin/tubulin represent the stability of dynamic MTs [43]. Tau protein, one of the major microtubule-associated proteins, can combine with tubulin to promote microtubule formation via polymerization effect. The expression of Tau reflects the amount of microtubules. As shown in Fig. 6A–C, the ratio of Ace-tubulin/ tubulin value and the expression levels of Tau protein were as follows: GFs-HP hydrogel group>Free GFs group>GFs-HP hydrogel group>PNI-diabetes group (Supplementary Table 1). GAP-43, a protein highly expressed in growth cones of developing and regenerating neurons, was tested in each group by western blotting. The result showed the same trend with the Tau protein (Fig. 6D. GFs-HP group vs. Free GFs group, P=0.004; GFs-HP group vs. PNI-diabetes group, P< 0.001; Free GFs group vs. PNI-diabetes group, P=0.004). Thus, GFs-HP hydrogel exerts positive effects on microtubule stabilization and augment the expression of functional proteins, allowing for sustained inducing axonal growth.

3.7. GFs-HP hydrogel facilitates SC proliferation

SCs are responsible for myelin formation and maintenance in the peripheral nervous system [11,44]. To verify that GFs-HP's facilitation of structural and functional recovery of injured sciatic nerve in diabetic was associated with SCs proliferation, immunocytochemical double-labelling analysis for Ki67 (a proliferation marker) and GFAP (marker of immature SCs) was evaluated in all experimental groups. Results showed that the fluorescence intensity of Ki67 was co-localized with the nuclei and surrounded within the GFAP in all groups, and the numbers of Ki67 positive cells was obviously increased in the Free GFs group when compared with the PNI-diabetes group. Furthermore, the GFs–HP hydrogel group showed significantly larger fluorescence intensity and many more Ki67 positive cells than the GFs group (Fig. 7A and B, 41.63±2.07% vs. 34.57±1.89%, P=0.040). In addition, the result of western blotting showed that the Free GFs group significantly increased the expression of Ki67 and proliferating cell nuclear antigen (PCNA, another typical cell proliferation marker), but to a lesser extent than the GFs-HP group (Fig. 7C–E, comparison between the GFs-HP group and Free GFs group: 0.44±0.02 vs. 0.34±0.02, P=0.005 for

Ki67 and 1.05±0.04 vs. 0.92±0.01, $P=0.027$ for PCNA). Collectively, these data suggest the beneficial role of GFs–HP hydrogel on nerve repair involves improved SCs proliferation.

3.8 Therapeutic effects of GFs–HP is linked with activation of MAPK/ERK, PI3K/Akt and JAK/STAT3 pathways

Phosphatidylinositol 3 kinase and protein kinase B (PI3K/Akt), janus kinase/signal transducer and activator of transcription (JAK/STAT3), and mitogen-activated protein kinase kinase/extracellular signal-regulated kinase (MAPK/ERK) are three common signaling pathways that regulate cell proliferation [45]. Activation of these distinct pathways correlates with neurotrophin participation [46,47]. To reveal the underlying mechanism by which GFs–HP hydrogel promotes SCs proliferation, the expression levels of *p*-AKT, AKT, *p*-ERK, ERK, *p*-STAT3, STAT3 of the lesioned sciatic nerves 30 days post-surgery were measured in each group by western blotting. As shown in Fig. 8A, the ratio of *p*-AKT/AKT, *p*-ERK/ERK, *p*-STAT3/STAT3 in the Free GFs and GFs–HP groups exhibited a marked increase compared with the PNI-diabetics group, and the percentage of the phosphorylation levels of AKT, ERK, and STAT3 in the GFs-HP hydrogel group showed the highest expression among the five groups, which were significantly higher than the Free GFs group (Fig. 8B, C and D: 0.47±0.02 vs. 0.35±0.02, $P = 0.005$ for *p*-AKT/AKT ratio, 5.42 ± 0.51 vs. 3.95 ± 0.30, $P = 0.047$ for *p*-ERK/ERK ratio and 0.60±0.04 vs. 0.47±0.02, $P=0.019$ for *p*-STAT3/STAT3 ratio, respectively). These data reveal that GFs–HP's administration may contribute to activations of the MAPK/ERK, PI3K/Akt, and JAK/STAT3 signal pathways, which is correlated with increased SCs proliferation.

4. Discussion

Restoring the functional reinnervation of injured peripheral nerves to near normal levels remains a challenging clinical problem, and patients are often subjected to partial or permanent disability of sensory and autonomic functions, especially for those are also suffering from chronic illnesses such as DM [1,48]. Molecular therapies using neurotrophic factors such as NGF and bFGF, the two most widely studied GFs, to promote peripheral nerve repair and regeneration have been investigated [49–51], however, maintaining appropriate spatial and temporal release of GFs are major hurdles to optimal efficacy. In this study, we demonstrated that co-administering NGF and bFGF loaded onto a heparin-poloxamer thermosensitive hydrogel (GFs-HP) via in situ injection efficiently and safely enhanced neuroprotection in diabetic rats suffering from peripheral nerve injury Additionally, the molecular mechanism of GFs-HP hydrogel's positive effect may involve the activations of MAPK/ERK, PI3K/Akt and JAK/STAT3 signaling pathways.

During nerve development and regeneration, the axonal sprouting and myelinated reformulation is not only dependent on intrinsic growth capability that involves complex sequences of molecular and cellular mechanisms, but also influenced by extrinsic factors that regulate the microenvironment of PNI [52,53]. An effective way to create an optimal microenvironment for nerve repair is supplying GFs and cytokines to the injured site [54]. NGF and bFGF, two extensively studied GFs of the neurotrophin family, have been shown to accelerate morphological and functional recovery in PNI and neurological disease [55].

Although both GFs can be endogenously synthesized and secreted by denervated neurons and SCs, their low expression levels are unable to induce survival and regrowth of damaged nerves [56,57]. Exogenous administration of GFs to lesioned areas has been well-studied, but most researches are focused on local administration a single GFs with or without materials to regulate spatial-temporal release of GFs. As proteinic drugs, bFGF and NGF are easily inactivated under physiological conditions, and their bioavailability varies dramatically in tissue and body fluids [58,59]. These shortcomings have required high-dosage and repetitive administration of bFGF or NGF, increasing the risk of undesirable reactions. High frequency of administration is disadvantageous for nerve repair, thus, seeking a delivery vehicle that can retain and release multiple GFs at lesion sites for an adequate period of time has been regarded to hold a great deal of promise for GFs-based therapeutics.

Poloxamer-based hydrogel offers an ideal drug delivery tool compatible with most living tissues and thus facilitates widespread application in neuroprotection and regeneration. For instance, a hydrogel incorporating poloxamer-407/188 polymer and monosialoganglio-side (GM1-hydrogel) was found be effective in preventing cell apoptosis and glial scar formation in rabbit spinal cord injuries (SCI) [60]. Recently, our group prepared a thermosensitive GFs hydrogel system for delivering single GFs directly to the lesion area of damaged nerves [26], which consists of poloxamer 407 and heparin through a poly-condensation reaction. Poloxamer 407 is a safe biocompatible polymer, and has been approved by U.S. Food and Drug Administration (FDA) for suture-less and atraumatic vascular anastomosis [61]. Heparin is a glycosaminoglycan formed by the alternation of two polysaccharides. Together, heparin-poloxamer copolymer have been shown to improve SCI repair and regeneration via inhibition of chronic endoplasmic reticulum (ER) stress-induced and autophagy-induced apoptosis [26,62]. The temperature-sensitive property of HP is suitable for in situ administration and has been applied for medical adhesive anastomosis [27,32]. At 4°C, HP is in a solution state, which is convenient for loading GFs. In vivo, HP transforms into a gel state at body temperature (37°C), which provides suitable mechanical strength and mediates a localized steady release of GFs over time. Furthermore, another key feature of heparin is its ability to bind a number of protein and peptides and prevent their hydrolytic degradation, making it a frequently used substance to modulate GFs bioactivity [63,64]. Thus, poloxamer 407 grafted with heparin helps to protect not only GFs activity and conformation, but also spatiotemporal controlled release of two GFs over a designated time-frame [27]. The current study’s use of heparin-based hydrogels to co-deliver bFGF and NGF holds several advantages: (i) Biosafety and biocompatibility of the hydrogel (documented in vitro and in vivo [26,62,65]). (ii) Encapsulation of multiple GFs and releasing them in a slow and sustained manner (Fig. 3A). (iii) Protection of GFs from enzymatic degradation. (iv) Temperature-sensitivity (Fig. 1) in favor of orthotopic administration in vivo. (v) Three-dimensional network structure (Fig. 2A) that allows GFs to load at a high amount. In the present study, we investigated the effect of 30-day consecutive administration of free GFs and the effect of single injection of GFs loaded onto HPs (GFs-HP), and showed that GF deliver via HP hydrogel is clearly superior in terms of neuroprotection, regeneration, and functional reinnervation. Our in vivo experiments also showed that delivering GFs via HP hydrogel is clearly efficacious in terms of neuroprotection, regeneration, and functional reinnervation. Our in vivo experiments also showed that one single in situ administration GFs-loaded HP hydrogel was sufficient to continuously promote axonal and myelinated reconstruction, neural tissue and gastrocnemius muscle regeneration, as well as motor function recovery after nerve crush injury in diabetic rats (Figs. 3–6), and the effect is markedly superior to consecutive free GFs injections. These results indicated that the neuroprotective effect of GFs could be enhanced after being loaded onto the heparin-based hydrogel.

The reasoning of co-administrating NGF and bGFG lies in the fact that single administration is largely suboptimal as nerve regeneration requires a multitude of steps that depend on different GFs in a time- and concentration-dependent fashion [66]. Here, for the first time, we combined multiple GFs to the injury site, which we hypothesize should have synergistic effects on nerve regeneration. Both NGF and bFGF have demonstrated neuroprotective and regenerative capacities for sustaining neural growth and extension after prolonged denervation [67,68], however, bFGF is also an angiogenic inducer that strongly stimulates vessel sprouting and remodeling around the lesion region of injured nerve, which can contribute to axon regrowth and repair by enhancing transit of more nutrients and relieving toxic metabolites [69]. Thus, incorporating multiple GFs into injured nerve stump via a regulated spatial temporal method might be a superior and promising therapy for more efficient and effective nerve regeneration. In the present study, we demonstrated that the co-application of bFGF and NGF loaded onto an HP hydrogel led to a robust neuroprotective response with extensive generation of new myelin en-sheathing axons at the nerve lesion site in diabetic rats. Compared with the PNI-diabetic group, the expression levels of MT-associated proteins and intracellular growth associated proteins were significantly increased, reflecting microtubule stabilization and growth cone formation. Moreover, gastrocnemius atrophy and motor function impairment of the sciatic nerve were markedly attenuated with GFs-HP treatment. Therefore, our works show that when combined with spatial-temporal regulation via HP hydrogel, co-application of NGF and bFGF may synergistically induce the micro-structural alterations that enhance overall functional recovery of injured sciatic nerves in diabetic rats.

Nerve injury results in SCs dedifferentiation and proliferation, causing SCs to be confined to the basal lamina to form Büngner bands, which is an essential process for axonal repair and myelin regrowth [70,71]. Once proliferating, SCs contact the regenerative axons, redifferentiate to ensheath axon, and form myelin. Thus, promoting SCs proliferation in the distal lesion segment is crucial for the development and functional recovery of peripheral nerves [72]. In this study, our results showed a robustly enhanced activity of SCs proliferation after the application of dual GFs, especially when loaded onto the HP hydrogel (Fig. 7). This suggests that co-delivery of bFGF and NGF via a slow-release HP hydrogel platform may be a potent promoter of SC proliferation in peripheral regeneration following PNI.

The primary biological actions of GF signaling is pivotal to mount a proliferative response for SCs [73]. Recently, MAPK/ERK, PI3K/Akt, and JAK/STAT3 signaling pathways that regulate naturally-occurring cell proliferation have been identified following nerve injury in mammals [74,75]. In spinal cord injury models, neuregulin-1-erbB activating microglial proliferation was dependent on the MAPK/ERK pathway [76]. Zuo et al. found that gastrodin effectively promoted proliferation and migration of RSC96cells by regulating gene expression of PI3K/Akt and ERK1/2 phosphorylation [77]. JAK/STAT3 is also an important regulator of neurotrophin growth factor signaling in neurite outgrowth [47]. To explore whether GFs-HP led to SCs proliferation following nerve injury via activation of these three signaling pathways, we explored the phosphorylation of AKT, ERK and STAT3 by western blotting. Our in vivo research demonstrated that bFGF and NGF combination therapy, especially when loaded onto an HP hydrogel, is clearly associated with increased phosphorylation of AKT, ERK, and STAT3 (Fig. 8), indicating that these three signaling pathways are activated following therapy. Combined with the observed SCs proliferation and differentiation enhancement, we hypothesize that GFs–HP's administration may contribute to activations of the MAPK/ERK, PI3K/Akt, and JAK/STAT3 signal pathways, which is correlated with increased SCs proliferation. Further investigations via culturing primary SCs in high glucose conditions are necessary to verify this mechanistic relationship.

While we believe that our results show that in situ GFs-HP administration has great potential for peripheral nerve regeneration, this study carries several limitations. First, we do not have electrophysiology data to evaluate motor functional recovery after sciatic nerve injury. Electrophysiology assessment is an effective method to evaluate functional recovery of the regenerated sciatic nerve. These methods were widely adopted in many research papers [78–80], including our previous studies [81–83]. However, it also carries several limitations, including the need for larger sample sizes (therefore more animals) to obtain sufficient statistical power due to the high variance of measurements. Second, while our results indicate that the therapeutic effects of GFs-HP likely involve promoting axonal regeneration and increasing myelination of surviving fibers, performing the immunofluorescence studies at additional time points may provide information about temporal morphological changes with hydrogel-GF treatment. However, our results can be used to demonstrate the superior therapeutic effect of single injection of GFs-HP hydrogel for 30-day treatment of sciatic nerve injury in diabetic rats compared to 30 days of consecutive injection of equal free GFs. Moreover, from the result of SFI values and BBB evaluation, we can conclude that the controlled released of GFs-HP is also beneficial for motor functional recovery. Third, we did not investigate the effect of single NGF or bFGF administration, thus, whether combining NGF and bFGF has synergistic effects is not fully known. The individual effect of bFGF and NGF has been validated in our prior studies [33,84]. Studies have indicated that co-administration of NGF and bFGF together could synergistically promote tissue reinnervation and neural differentiation, compared with bFGF and NGF alone [85,86]. In this study, we evaluated the effectiveness of dual GF administration for the first time in peripheral nerve injuries, and focused on showing how HP hydrogel can augment this therapy strategy. Further studies involving electrophysiology measurements, temporal changes in tissue morphology, and comparisons of single vs. multiple GF administration may be needed to fully elaborate the effectiveness of the GFs-HP technology.

5. Conclusion

In summary, heparin-based hydrogel is a promising vehicle for localized, controlled delivery of multiple GFs by self-assembly. A single-dose HP hydrogel treatment with of bFGF and

NGF (15μg each) resulted in beneficial effects on motor recovery, axon and myelin rehabilitation and interaction, microtubule stabilization, and SC proliferation in diabetic rats with sciatic nerve injury. Furthermore, our mechanistic investigation also revealed GFs–HP's administration may contribute to activations of the MAPK/ERK, PI3K/Akt, and JAK/STAT3 signal pathways, which is correlated with increased SCs proliferation (Supplementary Fig. 3). Thus, controlled in situ delivery of GFs via HP hydrogel may be a promising therapeutic intervention for peripheral nerve regeneration.

Supplementary Material

Refer to Web version on PubMed Central for supplementary material.

Acknowledgments

This study was partially supported by a research grant from the National Natural Science Funding of China (81372112, 81572237), Zhejiang Provincial Natural Science Foundation of China (Q18H090037, LY17H090017, LQ15E030003), Wenzhou Municipal Science & Technology Bureau of China (Y20140574). XJ was partially supported by Maryland Stem Cell Research Fund, USA (2013-MSCRFE-146-00, 2018-MSCRFD-4271) (both to XJ), and R01HL118084 from United States National Institutes of Health (NIH) (to XJ).

References

1. Pabari A, Yang SY, Seifalian AM, Mosahebi A. Modern surgical management of peripheral nerve gap. J Plast Reconstr Aesthetic Surg : JPRAS. 2010; 63:1941–1948.
2. Konofaos P, Ver Halen JP. Nerve repair by means of tubulization: past, present, future. J Reconstr Microsurg. 2013; 29:149–164. [PubMed: 23303520]
3. Noble J, Munro CA, Prasad VS, Midha R. Analysis of upper and lower extremity peripheral nerve injuries in a population of patients with multiple injuries. J Trauma. 1998; 45:116–122. [PubMed: 9680023]
4. Guariguata L, Whiting DR, Hambleton I, Beagley J, Linnenkamp U, Shaw JE. Global estimates of diabetes prevalence for 2013 and projections for 2035. Diabetes Res Clin Pract. 2014; 103:137–149. [PubMed: 24630390]
5. Whiting DR, Guariguata L, Weil C, Shaw J. IDF diabetes atlas: global estimates of the prevalence of diabetes for 2011 and 2030. Diabetes Res Clin Pract. 2011; 94:311–321. [PubMed: 22079683]
6. Callaghan BC, Cheng HT, Stables CL, Smith AL, Feldman EL. Diabetic neuropathy: clinical manifestations and current treatments. Lancet Neurol. 2012; 11:521–534. [PubMed: 22608666]
7. Zenker J, Ziegler D, Chrast R. Novel pathogenic pathways in diabetic neuropathy. Trends in Neurosciences. 2013; 36:439. [PubMed: 23725712]
8. Szalai E, Deak E, Modis L Jr, Nemeth G, Berta A, Nagy A, et al. Early corneal cellular and nerve fiber pathology in young patients with type 1 diabetes mellitus identified using corneal confocal microscopy. Investig Ophthalmol Vis Sci. 2016; 57:853–858. [PubMed: 26943147]
9. Kennedy JM, Zochodne DW. The regenerative deficit of peripheral nerves in experimental diabetes: its extent, timing and possible mechanisms. Brain J Neurol. 2000; 123(Pt 10):2118–2129.
10. Schulte-Herbruggen O, Braun A, Rochlitzer S, Jockers-Scherubl MC, Hellweg R. Neurotrophic factors–a tool for therapeutic strategies in neurological, neuropsychiatric and neuroimmunological diseases? Curr Med Chem. 2007; 14:2318–2329. [PubMed: 17896980]
11. Allodi I, Udina E, Navarro X. Specificity of peripheral nerve regeneration: interactions at the axon level. Prog Neurobiol. 2012; 98:16–37. [PubMed: 22609046]
12. Dey I, Midha N, Singh G, Forsyth A, Walsh SK, Singh B, et al. Diabetic Schwann cells suffer from nerve growth factor and neurotrophin-3 underproduction and poor associability with axons. Glia. 2013; 61:1990–1999. [PubMed: 24123456]

13. Grosheva M, Nohroudi K, Schwarz A, Rink S, Bendella H, Sarikcioglu L, et al. Comparison of trophic factors' expression between paralyzed and recovering muscles after facial nerve injury. A quantitative analysis in time course. Exp Neurol. 2016; 279:137–148. [PubMed: 26940083]
14. Apfel SC. Neurotrophic factors and diabetic peripheral neuropathy. Eur Neurol. 1999; 41(Suppl 1): 27–34. [PubMed: 10023126]
15. Cui Y, Lu C, Meng D, Xiao Z, Hou X, Ding W, et al. Collagen scaffolds modified with CNTF and bFGF promote facial nerve regeneration in minipigs. Biomaterials. 2014; 35:7819–7827. [PubMed: 24930851]
16. Skaper SD. The neurotrophin family of neurotrophic factors: an overview. Meth Mol Biol. 2012; 846:1–12.
17. Davis JB, Stroobant P. Platelet-derived growth factors and fibroblast growth factors are mitogens for rat Schwann cells. J Cell Biol. 1990; 110:1353–1360. [PubMed: 2157720]
18. Li GD, Wo Y, Zhong MF, Zhang FX, Bao L, Lu YJ, et al. Expression of fibroblast growth factors in rat dorsal root ganglion neurons and regulation after peripheral nerve injury. Neuroreport. 2002; 13:1903–1907. [PubMed: 12395088]
19. Chu H, Gao J, Chen CW, Huard J, Wang Y. Injectable fibroblast growth factor-2 coacervate for persistent angiogenesis. Proc Natl Acad Sci USA. 2011; 108:13444–13449. [PubMed: 21808045]
20. Andrades JA, Wu LT, Hall FL, Nimni ME, Becerra J. Engineering, expression, and renaturation of a collagen-targeted human bFGF fusion protein. Growth Factors. 2001; 18:261–275. [PubMed: 11519825]
21. Lane JT. The role of retinoids in the induction of nerve growth factor: a potential treatment for diabetic neuropathy. Transl Res J Lab Clin Med. 2014; 164:193–195.
22. Kemp SW, Webb AA, Dhaliwal S, Syed S, Walsh SK, Midha R. Dose and duration of nerve growth factor (NGF) administration determine the extent of behavioral recovery following peripheral nerve injury in the rat. Exp Neurol. 2011; 229:460–470. [PubMed: 21458449]
23. Karamoysoyli E, Burnand RC, Tomlinson DR, Gardiner NJ. Neuritin mediates nerve growth factor-induced axonal regeneration and is deficient in experimental diabetic neuropathy. Diabetes. 2008; 57:181–189. [PubMed: 17909094]
24. Tsai CC, Lu MC, Chen YS, Wu CH, Lin CC. Locally administered nerve growth factor suppresses ginsenoside Rb1-enhanced peripheral nerve regeneration. Am J Chin Med. 2003; 31:665–673. [PubMed: 14696670]
25. Rapraeger AC, Krufka A, Olwin BB. Requirement of heparan sulfate for bFGF-mediated fibroblast growth and myoblast differentiation. Science. 1991; 252:1705–1708. [PubMed: 1646484]
26. Zhao YZ, Jiang X, Xiao J, Lin Q, Yu WZ, Tian FR, et al. Using NGF heparin-poloxamer thermosensitive hydrogels to enhance the nerve regeneration for spinal cord injury. Acta Biomater. 2016; 29:71–80. [PubMed: 26472614]
27. Zhao YZ, Lv HF, Lu CT, Chen LJ, Lin M, Zhang M, et al. Evaluation of a novel thermosensitive heparin-poloxamer hydrogel for improving vascular anastomosis quality and safety in a rabbit model. PLoS One. 2013; 8:e73178. [PubMed: 24015296]
28. Ma F, Xiao Z, Chen B, Hou X, Dai J, Xu R. Linear ordered collagen scaffolds loaded with collagen-binding basic fibroblast growth factor facilitate recovery of sciatic nerve injury in rats. Tissue Eng. 2014; 20:1253.
29. Dinis TM, Elia R, Vidal G, Auffret A, Kaplan DL, Egles C. Method to form a fiber/growth factor dual-gradient along electrospun silk for nerve regeneration. ACS Appl Mater Interfaces. 2014; 6:16817–16826. [PubMed: 25203247]
30. Madduri S, di Summa P, Papaloizos M, Kalbermatten D, Gander B. Effect of controlled co-delivery of synergistic neurotrophic factors on early nerve regeneration in rats. Biomaterials. 2010; 31:8402–8409. [PubMed: 20692034]
31. Chen FM, Zhang M, Wu ZF. Toward delivery of multiple growth factors in tissue engineering. Biomaterials. 2010; 31:6279–6308. [PubMed: 20493521]
32. Tian JL, Zhao YZ, Jin Z, Lu CT, Tang QQ, Xiang Q, et al. Synthesis and characterization of Poloxamer 188-grafted heparin copolymer. Drug Dev Ind Pharm. 2010; 36:832–838. [PubMed: 20515404]

33. Zhang H, Wu F, Kong X, Yang J, Chen H, Deng L, et al. Nerve growth factor improves functional recovery by inhibiting endoplasmic reticulum stress-induced neuronal apoptosis in rats with spinal cord injury. J Transl Med. 2014; 12:130. [PubMed: 24884850]
34. Coppey LJ, Gellett JS, Davidson EP, Dunlap JA, Lund DD, Yorek MA. Effect of antioxidant treatment of streptozotocin-induced diabetic rats on en doneurial blood flow, motor nerve conduction velocity, and vascular reactivity of epineurial arterioles of the sciatic nerve. Diabetes. 2001; 50:1927–1937. [PubMed: 11473057]
35. Li R, Wu J, Lin Z, Nangle MR, Li Y, Cai P, et al. Single injection of a novel nerve growth factor coacervate improves structural and functional regeneration after sciatic nerve injury in adult rats. Exp Neurol. 2017; 288:1–10. [PubMed: 27983992]
36. Mohammadi R, Sanaei N, Ahsan S, Masoumi-Verki M, Khadir F, Mokarizadeh A. Stromal vascular fraction combined with silicone rubber chamber improves sciatic nerve regeneration in diabetes. Chinese Journal of Traumatology = Zhonghua chuang shang za zhi. 2015; 18:212–218. [PubMed: 26764542]
37. Bain JR, Mackinnon SE, Hunter DA. Functional evaluation of complete sciatic, peroneal, and posterior tibial nerve lesions in the rat. Plast Reconstr Surg. 1989; 83:129–138. [PubMed: 2909054]
38. Du J, Chen H, Zhou K, Jia X. Quantitative multimodal evaluation of passaging human neural crest stem cells for peripheral nerve regeneration. Stem Cell Rev. 2018; 14:92–100. [PubMed: 28780695]
39. Chen H, Du J, Zhang Y, Barnes K, Jia X. Establishing a reliable gait evaluation method for rodent studies. J Neurosci Meth. 2017; 283:92–100.
40. Wang Q, He Y, Zhao Y, Xie H, Lin Q, He Z, et al. A Thermosensitive heparin-poloxamer hydrogel bridge aFGF to treat spinal cord injury. ACS Appl Mater Interfaces. 2017; 9:6725. [PubMed: 28181797]
41. Kahn OI, Baas PW. Microtubules and growth cones: motors drive the turn. Trends in Neurosciences. 2016; 39:433–440. [PubMed: 27233682]
42. Tanaka E, Ho T, Kirschner MW. The role of microtubule dynamics in growth cone motility and axonal growth. J Cell Biol. 1995; 128:139–155. [PubMed: 7822411]
43. Witte H, Neukirchen D, Bradke F. Microtubule stabilization specifies initial neuronal polarization. J Cell Biol. 2008; 180:619–632. [PubMed: 18268107]
44. Brugger V, Duman M, Bochud M, Munger E, Heller M, Ruff S, et al. Delaying histone deacetylase response to injury accelerates conversion into repair Schwann cells and nerve regeneration. Nat Commun. 2017; 8:14272. [PubMed: 28139683]
45. Li B, Qiu T, Iyer KS, Yan Q, Yin Y, Xie L, et al. PRGD/PDLLA conduit potentiates rat sciatic nerve regeneration and the underlying molecular mechanism. Biomaterials. 2015; 55:44–53. [PubMed: 25934451]
46. Dominguez E, Rivat C, Pommier B, Mauborgne A, Pohl M. JAK/STAT3 pathway is activated in spinal cord microglia after peripheral nerve injury and contributes to neuropathic pain development in rat. J Neurochem. 2008; 107:50–60. [PubMed: 18636982]
47. Quarta S, Baeumer BE, Scherbakov N, Andratsch M, Rose-John S, Dechant G, et al. Peripheral nerve regeneration and NGF-dependent neurite outgrowth of adult sensory neurons converge on STAT3 phosphorylation downstream of neuropoietic cytokine receptor gp130. J Neurosci : the official Journal of the Society for Neuroscience. 2014; 34:13222–13233.
48. Moore AM, Kasukurthi R, Magill CK, Farhadi HF, Borschel GH, Mackinnon SE. Limitations of conduits in peripheral nerve repairs. Hand. 2009; 4:180–186. [PubMed: 19137378]
49. Xiao N, Le QT. Neurotrophic factors and their potential applications in tissue regeneration. Arch Immunol Ther Exp. 2016; 64:89–99.
50. Wood MD, Hunter D, Mackinnon SE, Sakiyama-Elbert SE. Heparin-binding-affinity-based delivery systems releasing nerve growth factor enhance sciatic nerve regeneration. J Biomater Sci Polym Ed. 2010; 21:771–787. [PubMed: 20482984]
51. Oliveira SL, Pillat MM, Cheffer A, Lameu C, Schwindt TT, Ulrich H. Functions of neurotrophins and growth factors in neurogenesis and brain repair. Cytometry Part A : the journal of the International Society for Analytical Cytology. 2013; 83:76–89. [PubMed: 23044513]

52. Forbes SJ, Rosenthal N. Preparing the ground for tissue regeneration: from mechanism to therapy. Nat Med. 2014; 20:857–869. [PubMed: 25100531]
53. Gurtner GC, Werner S, Barrandon Y, Longaker MT. Wound repair and regeneration. Nature. 2008; 453:314–321. [PubMed: 18480812]
54. Giannaccini M, Calatayud MP, Poggetti A, Corbianco S, Novelli M, Paoli M, et al. Magnetic nanoparticles for efficient delivery of growth factors: stimulation of peripheral nerve regeneration. Advanced Healthcare Materials. 2017; 6
55. English AW, Wilhelm JC, Ward PJ. Exercise, neurotrophins, and axon regeneration in the PNS. Physiology. 2014; 29:437–445. [PubMed: 25362637]
56. Gordon T. Neurotrophic factor expression in denervated motor and sensory Schwann cells: relevance to specificity of peripheral nerve regeneration. Exp Neurol. 2014; 254:99–108. [PubMed: 24468476]
57. Sebert ME, Shooter EM. Expression of mRNA for neurotrophic factors and their receptors in the rat dorsal root ganglion and sciatic nerve following nerve injury. J Neurosci Res. 1993; 36:357. [PubMed: 8271314]
58. Tayalia P, Mooney DJ. Controlled growth factor delivery for tissue engineering. Adv Mater (Weinheim, Ger). 2009; 21:3269–3285.
59. Xu H, Yan Y, Li S. PDLLA/chondroitin sulfate/chitosan/NGF conduits for peripheral nerve regeneration. Biomaterials. 2011; 32:4506–4516. [PubMed: 21397324]
60. Liu D, Jiang T, Cai W, Chen J, Zhang H, Hietala S, et al. An in situ gelling drug delivery system for improved recovery after spinal cord injury. Advanced Healthcare Materials. 2016; 5:1513–1521. [PubMed: 27113454]
61. Chang EI, Galvez MG, Glotzbach JP, Hamou CD, Elftesi S, Rappl-eye CT, et al. Vascular anastomosis using controlled phase transitions in poloxamer gels. Nat Med. 2011; 17:1147–1152. [PubMed: 21873986]
62. Zhao YZ, Jiang X, Lin Q, Xu HL, Huang YD, Lu CT, et al. Thermosensitive heparin-poloxamer hydrogels enhance the effects of GDNF on neuronal circuit remodelling and neuroprotection after spinal cord injury. J Biomed Mater Res. 2018; 105:2816–2829.
63. Liang Y, Kiick KL. Heparin-functionalized polymeric biomaterials in tissue engineering and drug delivery applications. Acta Biomater. 2014; 10:1588–1600. [PubMed: 23911941]
64. Wijelath E, Namekata M, Murray J, Furuyashiki M, Zhang S, Coan D, et al. Multiple mechanisms for exogenous heparin modulation of vascular endothelial growth factor activity. J Cell Biochem. 2010; 111:461–468. [PubMed: 20524207]
65. Wang Q, He Y, Zhao Y, Xie H, Lin Q, He Z, et al. A thermosensitive heparin-poloxamer hydrogel bridges aFGF to treat spinal cord injury. ACS Appl Mater Interfaces. 2017; 9:6725–6745. [PubMed: 28181797]
66. Gordon, T. Chapter 61-The Biology, Limits, and Promotion of Peripheral Nerve Regeneration in Rats and Humans. Elsevier Ltd; 2015.
67. Skaper SD. The neurotrophin family of neurotrophic factors: an overview. Meth Mol Biol. 2012; 846:1.
68. Letourneau PC. Chemotactic response of nerve fiber elongation to nerve growth factor. Dev Biol. 1978; 66:183–196. [PubMed: 751835]
69. Sun D, Liu Y, Yu Q, Zhou Y, Zhang R, Chen X, et al. The effects of luminescent ruthenium(II) polypyridyl functionalized selenium nanoparticles on bFGF-induced angiogenesis and AKT/ERK signaling. Biomaterials. 2013; 34:171–180. [PubMed: 23059005]
70. Gaudet AD, Popovich PG, Ramer MS. Wallerian degeneration: gaining perspective on inflammatory events after peripheral nerve injury. J Neuroinflammation. 2011; 8:110. [PubMed: 21878126]
71. Nave KA. Myelination and support of axonal integrity by glia. Nature. 2010; 468:244–252. [PubMed: 21068833]
72. Jessen KR, Mirsky R. The repair Schwann cell and its function in regenerating nerves. J Physiol. 2016; 594:3521–3531. [PubMed: 26864683]
73. Mar FM, Bonni A, Sousa MM. Cell intrinsic control of axon regeneration. EMBO Rep. 2014; 15:254–263. [PubMed: 24531721]

74. Mar FM, Simoes AR, Rodrigo IS, Sousa MM. Inhibitory injury signaling represses axon regeneration after dorsal root injury. Mol Neurobiol. 2016; 53:4596–4605. [PubMed: 26298667]
75. Glenn TD, Talbot WS. Signals regulating myelination in peripheral nerves and the Schwann cell response to injury. Curr Opin Neurobiol. 2013; 23:1041–1048. [PubMed: 23896313]
76. Calvo M, Zhu N, Grist J, Ma Z, Loeb JA, Bennett DL. Following nerve injury neuregulin-1 drives microglial proliferation and neuropathic pain via the MEK/ERK pathway. Glia. 2011; 59:554–568. [PubMed: 21319222]
77. Zuo W, Xu F, Zhang K, Zheng L, Zhao J. Proliferation-enhancing effects of gastrodin on RSC96 Schwann cells by regulating ERK1/2 and PI3K signaling pathways. Biomedicine & Pharmacotherapy = Biomedecine & Pharmacotherapie. 2016; 84:747–753. [PubMed: 27710899]
78. Du J, Liu J, Yao S, Mao H, Peng J, Sun X, et al. Prompt peripheral nerve regeneration induced by a hierarchically aligned fibrin nanofiber hydrogel. Acta Biomater. 2017; 55:296–309. [PubMed: 28412554]
79. Das S, Sharma M, Saharia D, Sarma KK, Sarma MG, Borthakur BB, et al. In vivo studies of silk based gold nano-composite conduits for functional peripheral nerve regeneration. Biomaterials. 2015; 62:66–75. [PubMed: 26026910]
80. Georgiou M, Golding JP, Loughlin AJ, Kingham PJ, Phillips JB. Engineered neural tissue with aligned, differentiated adipose-derived stem cells promotes peripheral nerve regeneration across a critical sized defect in rat sciatic nerve. Biomaterials. 2015; 37:242–251. [PubMed: 25453954]
81. Du J, Chen H, Zhou K, Jia X. Quantitative multimodal evaluation of passaging human neural crest stem cells for peripheral nerve regeneration. Stem Cell Rev. 2018; 14:92–100. [PubMed: 28780695]
82. Lewitus D, Vogelstein RJ, Zhen G, Choi YS, Kohn J, Harshbarger S, et al. Designing tyrosine-derived polycarbonate polymers for biodegradable regenerative type neural interface capable of neural recording. IEEE Trans Neural Syst Rehabil Eng. 2011; 19:204–212. [PubMed: 21147598]
83. Jia X, Zhen G, Puttgen A, Zhang J, Chen T. Improved long-term recording of nerve signal by modified intrafascicular electrodes in rabbits. Microsurgery. 2008; 28:173–178. [PubMed: 18286654]
84. Zhang HY, Wang ZG, Wu FZ, Kong XX, Yang J, Lin BB, et al. Regulation of autophagy and ubiquitinated protein accumulation by bFGF promotes functional recovery and neural protection in a rat model of spinal cord injury. Mol Neurobiol. 2013; 48:452–464. [PubMed: 23516099]
85. Kim TH, Oh SH, An DB, Lee JY, Lee JH. Dual growth factor-immobilized microspheres for tissue reinnervation: in vitro and preliminary in vivo studies. J Biomater Sci Polym Ed. 2015; 26:322–337. [PubMed: 25597228]
86. Zhang J, Lian M, Cao P, Bao G, Xu G, Sun Y, et al. Effects of nerve growth factor and basic fibroblast growth factor promote human dental pulp stem cells to neural differentiation. Neurochem Res. 2017; 42:1015–1025. [PubMed: 28005222]

Appendix A. Supplementary data

Supplementary data related to this article can be found at https://doi.org/10.1016/j.biomaterials.2018.03.044.

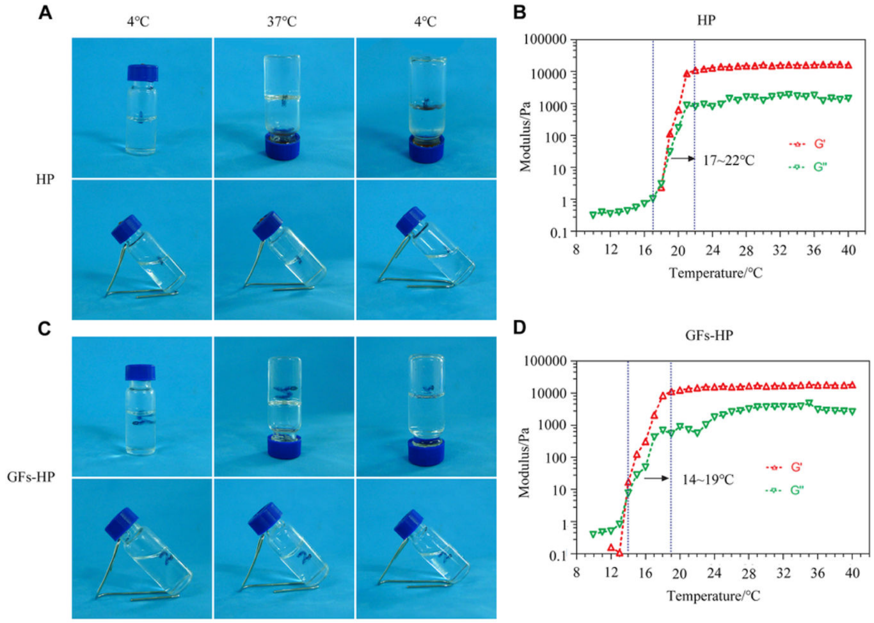

Fig. 1.

The thermosensitive property of GFs-HP hydrogel. A, C. Visualization of the state of HP and GFs-HP respectively at different temperatures (4°C, 37°C and 4°C after 37°C). At 37°C, both hydrogels are clearly in a gel state, while at 4°C before or after heating, both hydrogels are clearly in a sol state. B, D. Storage (G′) and loss (G″) moduli as rheological markers in temperatures ranging from 10 to 40°C for HP and GFs-HP hydrogels, respectively. Results show that the temperature of gel-sol phase transition for HP is slightly higher than that of GFs-HP, but both are well below 37°C.

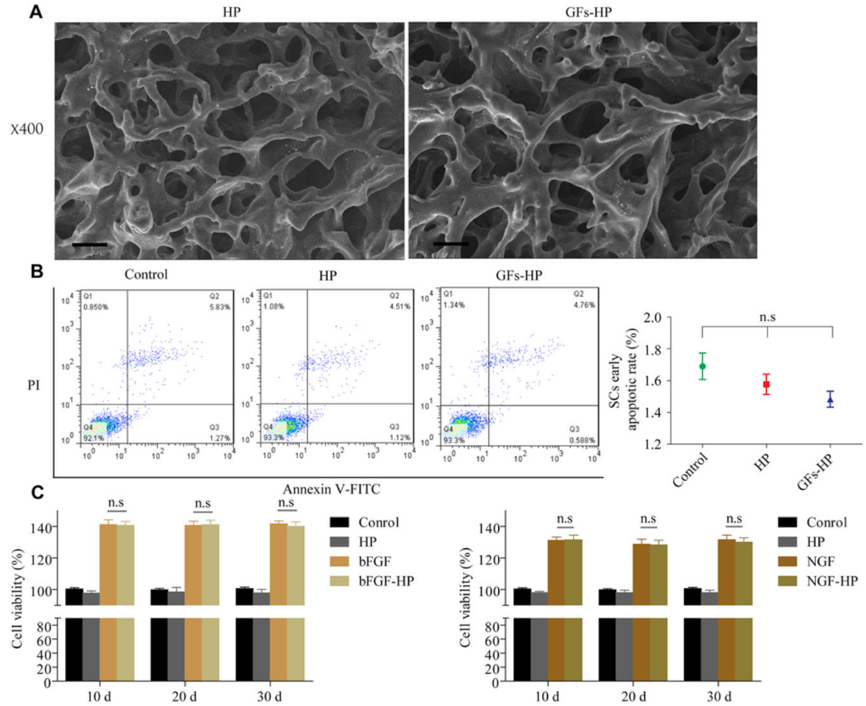

Fig. 2.

The microstructure and safety of HP-hydrogel with/without GFs. A. SEM image of the morphology HP and GFs-HP hydrogel. Scale bar=100μm; B. The survival rate of RSC96cells treated with HP with/without GFs using PI/annexin V-FITC staining and statistical results of early apoptosis rate. Results show that there is no appreciable change in apoptotic rate of SCs with GFs-HP hydrogel. n.s, nonsignifcant; C. The stability of the bFGF and NGF in the hydrogel at different times was evaluated by CCK-8 assay. All data represent mean values±SEM, n=3 for each group.

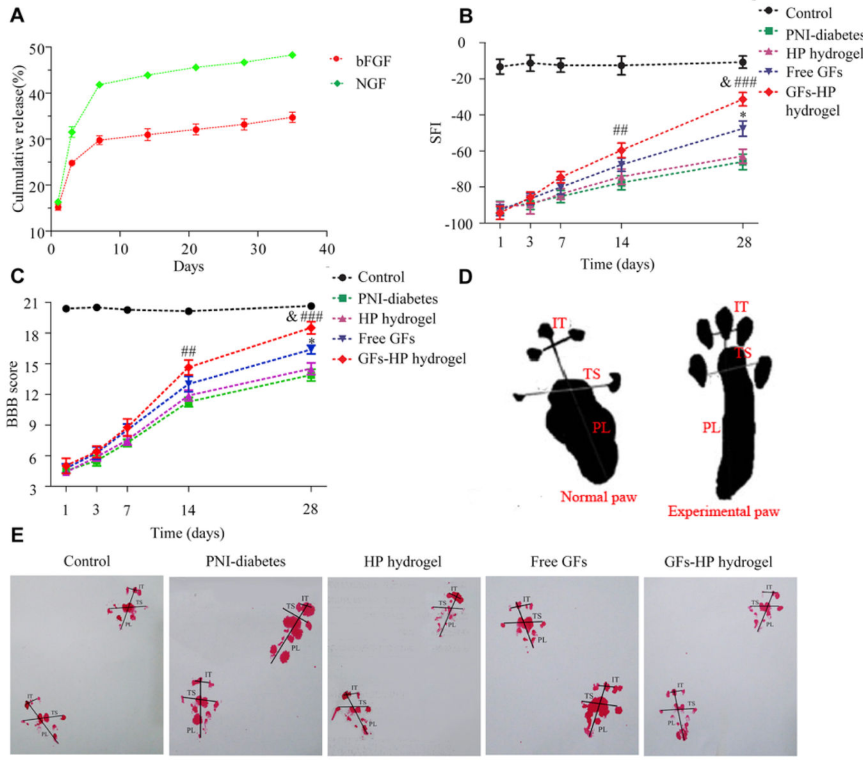

Fig. 3.

The continuous release of bFGF and NGF from GFs-HP hydrogel enhances motor functional recovery of the regenerated sciatic nerve. A. Release profile of encapsulated bFGF and NGF at different time points; B. The sciatic function index (SFI) values in all groups measured at the predetermined time postoperatively; C. Quantification of BBB scores in the indicated groups at the predetermined time postoperatively; D. A schematic for measuring parameters of footprints; E. Representative photographs of the rats' paw prints in each group 28 days after sciatic nerve crush injury. Free GFs vs PNI-diabetes: $^{*}P<0.05$, GFs-HP hydrogel vs PNI-diabetes: $^{\#\#}P<0.01$, $^{\#\#\#}P<0.001$, GFs-HP hydrogel vs Free GFs: $^{\&}P<0.05$. All data represent mean values±SEM, n=8 in each group.

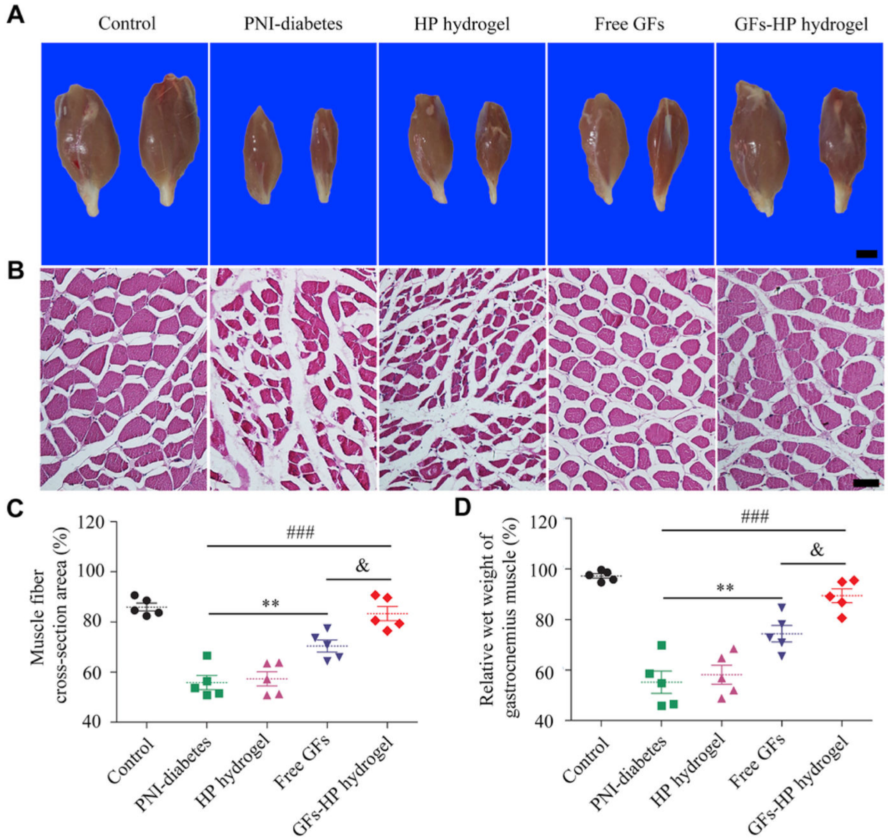

Fig. 4.

Analyses gastrocnemius muscle morphology and wet weight for evaluation of post-injury muscle atrophy. A, Representative photographs of gastrocnemius muscles from both hind limbs in each group. Scale bar, 25mm; B, Representative light microscopy images of cross-sectioned gastrocnemius muscles following H&E staining 30 days post-injury. Scale bar, 50μm; C. Histograms showing the percentage of cross-sectional area of muscle fibers quantified with Image-Pro Plus software analysis of light microscopy results; D. Wet weight ratios of gastrocnemius muscles in each group at 30 days post injury. Free GFs vs PNI-diabetes: $^{**}P<0.01$, GFs-HP hydrogel vs PNI-diabetes: $^{###}P<0.001$, GFs-HP hydrogel vs Free GFs: $^{\&}P<0.05$. All data represent mean values±SEM, n=5 for each group.

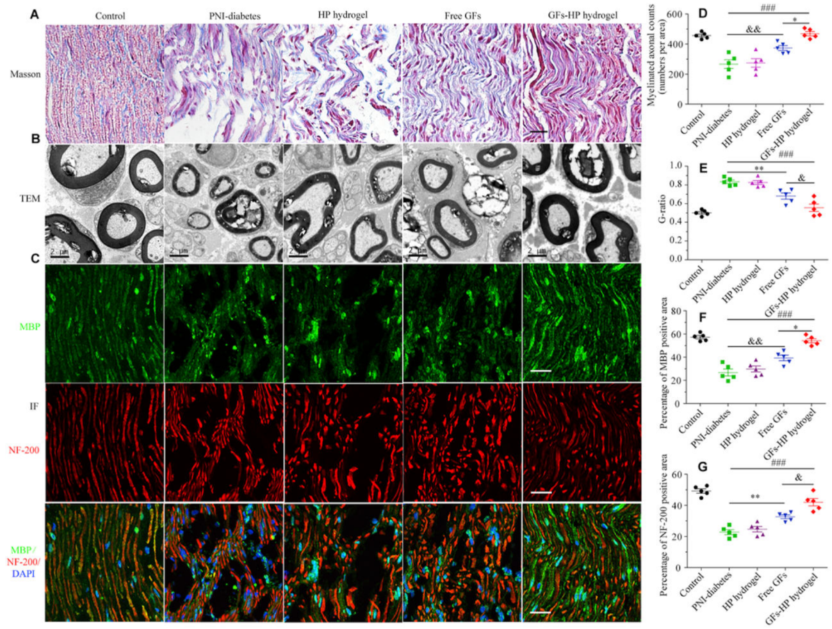

Fig. 5.

Histological and microstructure evaluation of injured sciatic nerve. A. longitudinal sections of regenerated nerve stained with Masson's trichrome 30 days after injury, Scale bar=50μm; B. TEM images of cross-sections of lesion regions, Scale bar=2μm; C. Double immunofluorescence staining for NF-200 and MBP-positive cells of the longitudinal sections in each experimental group. Scale bar=25μm; D, E. Quantification analysis of myelinated axonal count and G-ratio (G-ratio=axon diameter/fiber diameter) in the indicated groups; F, G. Quantitative analyses of fluorescence intensity of pixels for MBP and NF-200. Values are expressed as mean±SEM, n=5 per group. Free GFs vs PNI-diabetes: $^{*}P<0.05$, $^{**}P<0.01$, GFs-HP hydrogel vs PNI-diabetes: $^{\#\#\#}P<0.001$, GFs-HP hydrogel vs Free GFs: $^{\&}P<0.05$, $^{\&\&}P<0.01$.

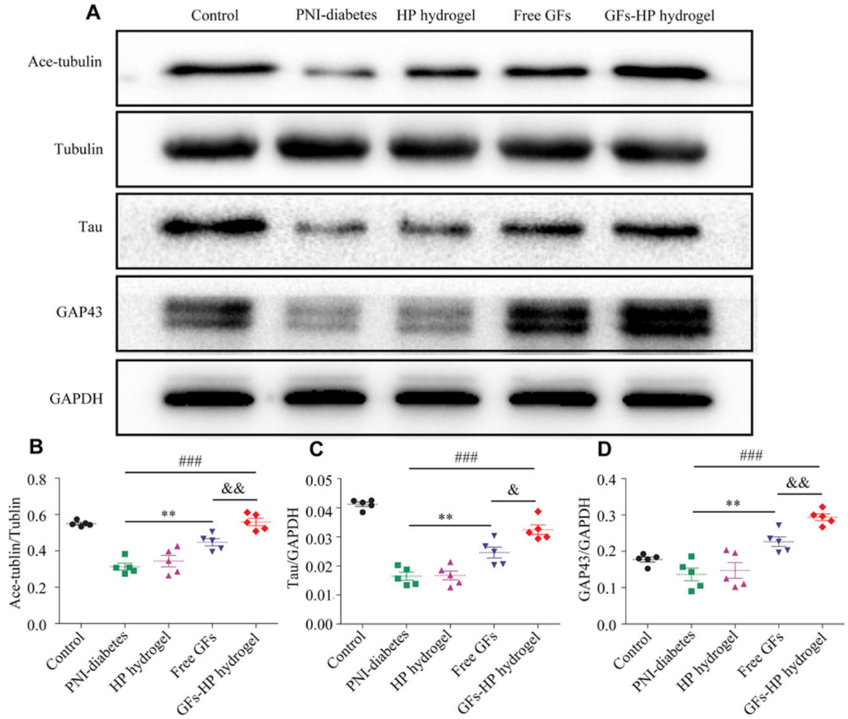

Fig. 6.

GFs-HP hydrogel maintains MT stability in axons and upregulates GAP43 expression. A. the expression levels of MT-associated proteins (Ace-tubulin, Tyr-tubulin, Tau) and neural structural protein GAP43 in sciatic nerve lesions from diabetic rats via western blotting (GAPDH served as a protein loading control); B, C, D. Densitometrical analysis of Ace-tubulin, Tyr-tubulin, Tau and GAP43, respectively. Data presented as mean±SEM, n=5 for each group. Free GFs vs PNI-diabetes: $^{**}P<0.01$, GFs-HP hydrogel vs PNI-diabetes: $^{###}P<0.001$, GFs-HP hydrogel vs Free GFs: $^{\&}P<0.05$, $^{\&\&}P<0.01$.

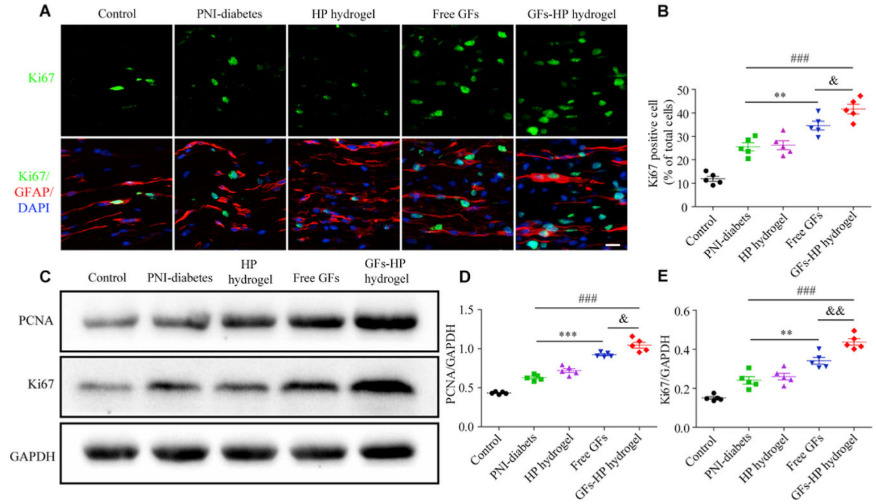

Fig. 7.

GFs-HP hydrogel facilitates SCs proliferation. A. The double immunofluorescence staining of Ki67 (green) with the GFAP (red) to label proliferating SCs in longitudinal sciatic nerve sections, Scale bar=50μm; B. The percentages of cells double-positive for Ki67 and GFAP out of total DAPI positive cells (representing proliferation rate of SCs); C. The protein levels of Ki67 and PCNA at 30 days after injury by western blotting; D, E. Densitometric analyses of PCNA and Ki67, respectively. GAPDH was used for band density normalization. Data presented as mean±SEM, n=5 for each group. Free GFs vs PNI-diabetes: $^{**}P<0.01$, $^{***}P<0.001$, GFs-HP hydrogel vs PNI-diabetes: $^{\#\#\#}$P<0.001, GFs-HP hydrogel vs Free GFs: $^{\&}P<0.05$, $^{\&\&}P<0.01$. (For interpretation of the references to color in this figure legend, the reader is referred to the Web version of this article.)

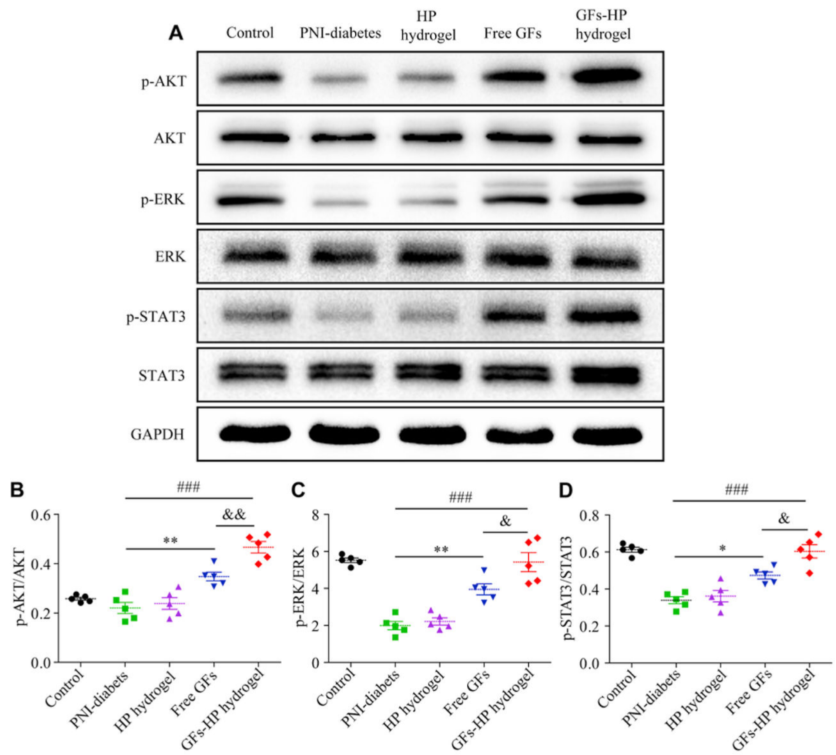

Fig. 8.

GFs-HP hydrogel treatment activates SCs proliferation through MAPK/ERK, PI3K/Akt and JAK/STAT3 pathways. A. Immunoblot for *p*-AKT, *p*-ERK, *p*-STAT3; total proteins amount of AKT, ERK, STAT3 served as loading control; B–D: Densitometric quantification of *p*-AKT/AKT, *p*-ERK/ERK and *p*-STAT3/STAT3, respectively. GAPDH was used for band density normalization. Data presented as Mean±SEM n=5 for each group. Significance markers: Free GFs vs PNI-diabetes: $^{*}P<0.05$, $^{**}P<0.01$, GFs-HP hydrogel vs PNI-diabetes: $^{\#\#\#}P<0.001$, GFs-HP hydrogel vs Free GFs: $^{\&}P<0.05$, $^{\&\&}P<0.01$.